Molecular & Cellular Toxicology (2020) 16:331–345
https://doi.org/10.1007/s13273-020-00075-9

ORIGINAL ARTICLE

Trichloroethylene injures rat liver and elevates the level of peroxisomal bifunctional enzyme (Ehhadh)

Nuanyuan Luo[1,2] · Qunqun Chang[1,2] · Xiaohu Ren[2] · Peiwu Huang[2] · Wei Liu[2] · Li Zhou[2] · Yungang Liu[1] · Jianjun Liu[2]

Accepted: 18 March 2020 / Published online: 2 April 2020

Abstract

Background Trichloroethylene (TCE) is a common industrial solvent and an occupational toxicant. TCE exposure can cause severe hepatotoxicity, but its mode of action is poorly understood. Many studies have shown TCE-induced liver damage in mice, while few have examined the effects of TCE in rats.

Objective To explore the effects of TCE in Sprague–Dawley (SD) rats and the potential mechanisms in TCE-induced hepatocytotoxicity.

Results The liver index and activities of liver damage marker enzymes (ALT, AST and ALP) in rat serum were elevated along with the increase in TCE dose, while the levels of total proteins and albumin in serum were reduced. The results suggest that TCE is hepatotoxic in rats. 2D-DIGE electrophoresis showed that the levels of 66 liver proteins in TCE-treated rats were abnormally altered (39 up-regulated and 27 down-regulated). In these proteins, six enzymes were related to liver damage and carcinogenesis as indicated by bioinformatics analysis, and Western blot analysis confirmed the alterations of three of them, i.e., aldehyde dehydrogenase 2 (Aldh2), glutathione S-transferase Mu 1 (Gstm1) and peroxisomal bifunctional enzyme (PBE, also named as Ehhadh). PBE was the only protein elevated in a dose dependent manner. Whether PBE can be a biomarker of TCE hepatotoxicity needs to be further studied.

Conclusion These findings indicate that TCE induces liver injury in rats.

Keywords Trichloroethylene · Peroxisomal bifunctional enzyme · Dose-dependent manner · Difference gel electrophoresis (DIGE) · MALDI-TOF MS/MS

Introduction

Trichloroethylene (TCE) is a chlorinated hydrocarbon widely used as a solvent in industrial applications. Because of inappropriate usage and transportation, TCE is now a major pollutant in soil and ground water (Wu and Schaum 2000). TCE exposure can cause severe toxic effects to humans, and the EPA (US Environmental Protection Agency) characterized TCE as carcinogenic in 2011 (Chiu et al. 2013). Exposure to TCE is therefore a human health risk in China and other regions of the world (Kamijima et al. 2007).

Liver is the major organ where TCE is typically metabolized into oxidative metabolites by cytochrome P450-dependent oxidation pathways. These metabolites play important roles in TCE-induced hepatotoxicity and carcinogenesis (Allemand et al. 1978; Lash et al. 2000). However, the precise mechanisms underlying TCE hepatotoxicity are unclear.

Nuanyuan Luo and Qunqun Chang contributed equally to this work.

✉ Yungang Liu
yungliu@126.com

✉ Jianjun Liu
junii8@126.com

[1] Department of Toxicology, School of Public Health, Guangdong Provincial Key Laboratory of Tropical Disease Research, Southern Medical University, Guangzhou 510515, Guangdong, China

[2] Key Laboratory of Modern Toxicology of Shenzhen, Shenzhen Medical Key Subject of Health Toxicology, Shenzhen Center for Disease Control and Prevention, No 8 Longyuan Road, Nanshan District, Shenzhen 518055, Guangdong, China

TCE appears to induce toxic responses in human hepatocytes (L-02 line) by dysregulating the expression of genes encoding CYP1A2 and BAX (BAX is associated with apoptosis) (Xu et al. 2012). Repeated administration of TCE to mice by oral gavage can produce hepatocellular proliferation, mitochondrial dysfunction and glycogen depletion (Sano et al. 2009). Proteome profiles of TCE-induced protein dysregulation in cultured hepatocytes indicate that specific proteins are related to TCE toxicity in human hepatocytes (Liu et al. 2007; Huang et al. 2009). Although there have been numerous studies on TCE-induced liver damage in either mouse in vivo or hepatocytes in vitro, few studies of TCE-induced toxicity in rat liver have been reported.

We studied TCE-induced liver toxicity in rats by exposing rats to TCE by gastric gavage and evaluating its effects on the liver. We then performed a comparative proteomics analysis, focusing on the profiles of liver proteins in TCE-treated SD rats. These studies were followed by analysis of the potential roles of the alterations in protein expression in TCE-induced liver toxicity.

Materials and methods

Animals and treatment

Male Sprague–Dawley (SD) rats, aged 7 weeks with body weights of 103–119 g, were purchased from the Experimental Animal Center of Guangdong Province (Guangzhou, China) and housed under specific pathogen-free (SPF) conditions. The animal experiments were approved by the Committee of Ethnics in the Shenzhen Center for Disease Control and Prevention. Animals were acclimatized to the laboratory conditions for 4 days prior to being randomly divided into four groups with ten rats per group. TCE was purchased from Sigma-Aldrich (Shanghai, China). The animals were fasted for 12 h before each administration, and food was provided 2 h after dosing. Tap water was available ad libitum. TCE was dissolved in corn oil at different doses (0, 250, 500 and 1000 mg/kg per day), with dosage being based on a previous report (Khan et al. 2009). TCE was administered by gastric gavage for 14 consecutive days. The body weight of each rat was recorded every other day during, and at the end of, the study. Animal care and treatments were performed in accordance with the Institutional Animal Care and the NIH Guide for the Care and Use of Laboratory Animals. At the end of the experiment (14 days), blood samples were collected and allowed to coagulate. The serum samples were then obtained and used for analyzing biochemical parameters. During necropsy, samples of liver tissue were taken, weighed and snap-frozen in liquid nitrogen to minimize proteolysis before storing at − 80 °C for analyses.

Serum biochemistry profile

The activities of alanine aminotransferase (ALT), aspartate aminotransferase (AST) and alkaline phosphatase (ALP), and the concentrations of total protein (TP) and albumin (ALB) in serum were analyzed using standard methodology (Bergmeyer et al. 1978), with commercially available kits obtained from Shanghai KEHUA bio-engineering (Shanghai, China). All analyses were performed on an Olympus AU 400 autoanalyzer (Hamburg, Germany).

Protein extraction and CyDye minimal labeling

Frozen liver samples were ground in liquid nitrogen and homogenized in a lysis buffer containing urea (7 M), thiourea (2 M), CHAPS [2% (w/v)], Tris (30 mM) and protease inhibitor cocktail (Thermo Scientific, Rockford, IL, USA). Homogenized samples were sonicated for 30 s, incubated on ice for 30 min and centrifuged at 20,000*g* for 30 min at 4 °C. Supernatants were precipitated with three volumes of ice-cold acetone at − 20 °C for 2 h, followed by centrifugation at 10,000*g* for 10 min at 4 °C. The resulting pellets were re-suspended in lysis buffer and centrifuged at 10,000*g* for 5 min. Protein concentrations of the supernatants were determined with the 2-D Quant kit (GE Healthcare, Pittsburgh, PA, USA) according to manufacturer instructions.

The purified samples were labeled with Cy2, Cy3 or Cy5 fluorescent dyes (200 pmol dyes per 25 µg protein) (GE healthcare, Pittsburgh, PA, USA) according to manufacturer instructions. Briefly, one half of individual samples from the same group were either labeled with Cy3 or Cy5 to avoid any dye-specific staining bias. An internal standard, made by pooling equal aliquots of all experimental samples, was labeled with Cy2. The labeling reaction was conducted on ice in darkness for 30 min and then quenched with 1 µL of 10 mM lysine (Sigma-Aldrich, Shanghai, China) for 10 min on ice shielded from light.

2D-DIGE electrophoresis

The Cy3- and Cy5-labeled samples were mixed together with an aliquot (25 µg) of Cy2-labeled internal standard. An equal volume of 2× sample buffer containing urea (7 M), thiourea (2 M), CHAPS [4% (w/v)], dithiothreitol [DTT, 2% (w/v)], and IPG buffer [2% (v/v), at pH 3–11] was added to each mixed sample and incubated on ice for 10 min prior to bringing the total sample volume to 450 µL with rehydration buffer (8 M of urea, 2% w/v of CHAPS, 0.28% w/v of DTT, 0.5% v/v of IPG Buffer at pH 3–10, and 0.002% w/v of bromophenol blue). Twelve differently pooled samples were loaded onto individual IPG strips (pH 3–11, nonlinear

gradient, 24 cm) (GE Healthcare, Pittsburgh, PA, USA) for isoelectric focusing (IEF) using an Ettan IPGphor 3 system (GE Healthcare, Pittsburgh, PA, USA). The IEF was programmed in the following five steps: 30 V for 12 h, 500 V for 1 h, 1000 V for 1 h, 8000 V gradient for 6 h, and then the unit was maintained at 8000 V until a total of 90,000 V-hours was reached. After IEF, the strips went through two steps of equilibration before applying on 12.5% SDS-PAGE gels. The second-dimension separation was conducted on an Ettan DALT six electrophoresis system (GE Healthcare, Pittsburgh, PA, USA) at 15 °C at 1 W per gel for 1 h, followed by 11 W per gel for 6 h. All electrophoresis procedures were performed in darkness.

Image acquisition and analysis

After electrophoresis, gels were immediately scanned by a Typhoon Trio Variable Mode Imager (GE Healthcare, Pittsburgh, PA, USA) at 100 µm resolution with excitation/emission wavelengths of 488 (Blue)/520, 532 (Green)/580 and 633 (Red)/670 nm for Cy2, Cy3 and Cy5, respectively. The images were processed by DeCyder 2D v6.5 (GE Healthcare, Pittsburgh, PA, USA) for differential analysis. Student's *t* test and one-way ANOVA were used to compare the strength of spots between each treatment and the control. Statistically significant spots ($p < 0.05$) with an average ratio ≥ 1.2 or ≤ -1.2 were marked for further analysis.

In-gel digestion and protein identification by MALDI-TOF–MS/MS

The significantly different protein spots were manually excised from a 2-DE gel stained with Coomassie brilliant blue G-250 staining solution. Gel plugs were de-stained with 50% acetonitrile in ammonium bicarbonate aqueous solution (25 mM) followed by dehydration in 100% acetonitrile. After removal of acetonitrile, each gel piece was digested overnight at 37 °C with 0.03 µg of sequencing-grade trypsin (Promega, Madison, WI, USA) in 15 µL of ammonium bicarbonate aqueous solution (25 mM). The extracted peptides were stored at − 80 °C prior to mass spectrometry analysis.

Peptides released from digestion were analyzed by an UltrafleXtreme MALDI-TOF/TOF mass spectrometer (Bruker Daltonics Inc., Billerica, MA, USA). Briefly, 2 µL of extracted peptide mixtures were spotted onto a polished steel MTP 384 target plate (Bruker Daltonics Inc., Billerica, MA, USA), air dried and covered with a 1 µL CHCA matrix (5 mg/mL in 50% ACN and 0.1% TFA). External calibration was performed using standard peptide calibration mixtures covering peaks between ~ 700 and 4000 Da (Bruker Daltonics Inc., Billerica, MA, USA). The peptide mass fingerprint (PMF) spectra were acquired in the positive reflection mode and the strongest seven peptides per spot were selected automatically for MS/MS analysis in LIFT mode. Protein identification by PMF and MS/MS spectra was performed using the Mascot search engine 2.2 (Matrix Science, Boston, MA, USA) and BioTools software (Bruker Daltonics Inc., Billerica, MA, USA). Confident matches in SwissProt database were defined by the Mascot score, the sequence coverage by matching peptides and statistical significance ($p < 0.05$).

Bioinformatics analysis

To determine the potential mechanisms mediating hepatotoxicity of TCE, PANTHER (http://pantherdb.org/) was used to classify protein families according to their cellular components, molecular functions and biological processes. STRING (http://string-db.org/, version 9.1) was used to identify protein networks of known and enrich proteins may be modulated in response to TCE exposure. Pathways with *p* values lower than 0.05 were considered to be significant (Franceschini et al. 2013).

Immunoblotting

To confirm the 2D-DIGE results, proteins with absolute values of average ratio > 1.2 and *t* values < 0.05 were selected for Western-blot analysis. Liver lysates were prepared with lysis buffer (Beyotime, Shanghai, China), homogenized, and centrifuged at 15,000*g* for 30 min. Extracts were mixed with protein loading buffer purchased from Thermo Scientific (Rockford, IL, USA) and heated for 5 min at 95 °C. The protein samples were separated by SDS-PAGE and transferred to PVDF membranes (Millipore, Darmstadt, Germany) in a semi-dry transfer unit (GE Healthcare, Pittsburgh, PA, USA). The blotted membranes were subsequently blocked in 5% (w/v) nonfat dry milk in TBS-T buffer (20 mM Tris–HCl, 150 mM NaCl, 0.2% Tween-20, pH 7.5) for 60 min. After being washed in TBS-T, the membranes were incubated with a mixture of several primary antibodies, including anti-GSTM1, anti-PBE, anti-β-Actin, anti-ALDH2, anti-CPS1, anti-ENO1, and anti-DDT antibodies (all from Boster Immunoleader, Pleasanton, CA, USA). After rewashing in TBS-T, the membranes were incubated with horseradish peroxidase-conjugated anti-rabbit IgG (Thermo Scientific, Rockford, IL, USA), and anti-goat IgG (Santa Cruz Biotechnology, CA, USA) secondary antibodies. The membranes were then developed using SuperSignal West Dura Substrate (Thermo Scientific, Rockford, IL, USA), and scanned with an Image Quant RT ECL scanner (GE Healthcare, Pittsburgh, PA, USA) for visualization of the proteins bound to the primary antibodies. The relative level of each

protein was calculated as a ratio between the grey value of the target band and that of the reference (β-actin).

Statistical analysis

The level of each observed parameter was expressed as mean ± standard deviation ($n = 10$) and analyzed by SPSS statistical software (version 20.0, Chicago, IL, USA). Differences between multiple groups were calculated using one-way ANOVA followed by a Dunnett's (two-sided) test. A $p < 0.05$ value was considered as statistically significant. Figures were generated by GraphPad Prism (version 7.0, GraphPad Software Inc., San Diego, CA, USA).

Results

TCE induces liver injury in rats

At terminal killing, the body weights of test animals in the TCE-treated groups and the control were similar ($p > 0.05$). However, the liver index significantly increased with the increase in TCE level (dose-dependence) (Table 1; Fig. 1). Additionally, the activities of the liver damage marker enzymes (ALT, AST and ALP) in the serum of TCE-treated rats increased significantly ($p < 0.001$, compared to the control), in a dose-dependent manner (Fig. 2). The total protein and albumin levels in serum in TCE-treated rats were both significantly ($p < 0.001$) lowered, compared with their levels in the control (Fig. 2).

Table 1 The influence of TCE on liver index in rats

TCE (mg/kg)	Body weight (g)	Liver weight (g)	Liver index[a]
0	155.1 ± 7.9	7.5 ± 0.8	4.8 ± 0.4
250	163.6 ± 6.4	9.0 ± 0.4***	5.5 ± 0.2**
500	162.2 ± 9.1	9.1 ± 0.8***	5.6 ± 0.4***
1000	159.7 ± 6.3	9.5 ± 0.5***	6.0 ± 0.4***

All values are expressed as mean ± SD

**$p < 0.01$, each TCE-exposure group vs the vehicle control (corn oil) group

***$p < 0.001$, each TCE-exposure group vs the vehicle control group

[a]Liver index = (Liver weight/body weight) × 100

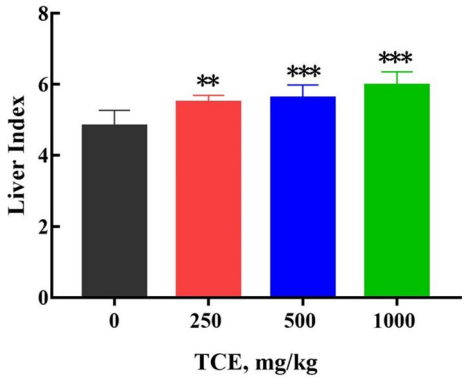

Fig. 1 Influence of TCE on the liver index of rats. Data are means and SD of ten replicates; **$p < 0.01$, compared with control; ***$p < 0.001$, compared with control

Differentially expressed proteins in the livers of TCE-exposed rats

To study the mechanism underlining TCE-induced hepatotoxicity, we evaluated the changes in the expression of hepatic proteins using 2D-DIGE. A total of 2000 protein spots were detected. Among these, 66 proteins were differentially expressed in TCE-treated rats (by one-way ANOVA, $p < 0.05$ combined with more than a 1.2-fold intensity difference) as identified by MALDI-TOF/TOF mass spectrometry (Fig. 3). The presence of different spots corresponding to the same protein was related to the occurrence of different isoforms, mainly due to post-translational modifications. Among the differentially expressed protein spots, 50 (belonging to 39 different proteins) were up-regulated, while 33 spots (27 different proteins) were down-regulated. The results of protein identification are summarized in Table 2.

Protein classification and functional analysis

PANTHER was used for protein classification analysis. Most of the differentially expressed proteins were mainly localized in the cytoplasm (63%) and mitochondrion (26%). The majority of proteins were associated with catalytic (68%) and binding activities (12%). Altered proteins were mainly involved in metabolic processes (55%) (Fig. 4).

Protein–protein interactions were analyzed by STRING (Franceschini et al. 2013). The data suggested a combined effect of these proteins in TCE-induced hepatotoxicity (Fig. 5). We categorized these proteins by their involvement in KEGG pathways ($p < 0.05$) using the "Enrichment" module integrated within STRING. As shown in Table 2, the pathways perturbed by TCE included fatty acid metabolism, PPAR signaling pathway, glycolysis/gluconeogenesis, and glutathione metabolism.

Verification of PBE as differentially expressed in TCE-induced hepatic injury

Six metabolic enzymes (aldehyde dehydrogenase (Aldh2), alpha-enolase (Eno1), D-dopachrome decarboxylase (Ddt), carbamoyl-phosphate synthase (Cps1), glutathione *S*-transferase Mu 1 (Gstm1) and peroxisomal bifunctional enzyme (PBE) appeared to be associated with TCE-induced

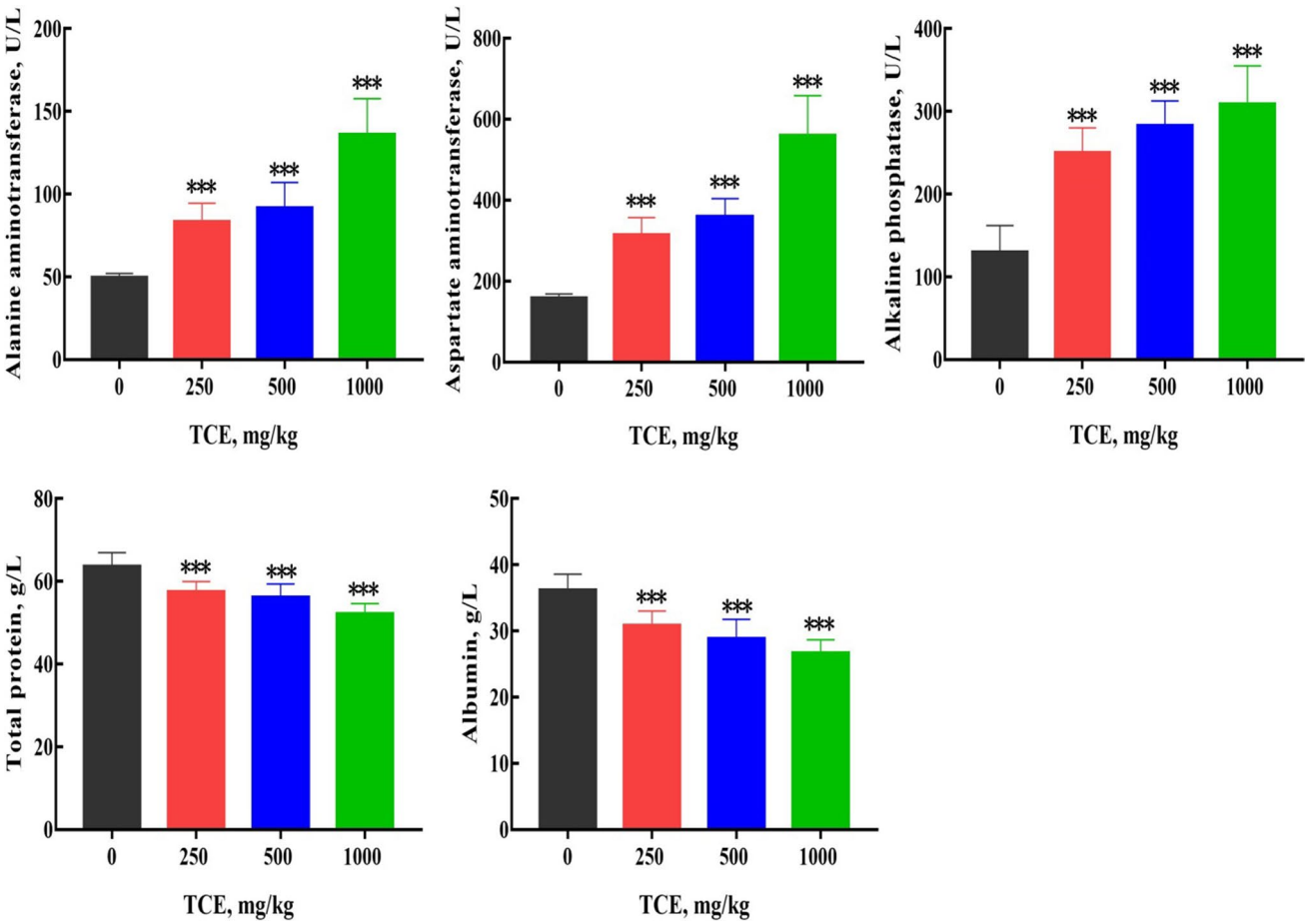

Fig. 2 Alterations of serum indicators of liver injury in SD rats exposed to TCE. See legend of Fig. 1; ***$p < 0.001$, compared with the control

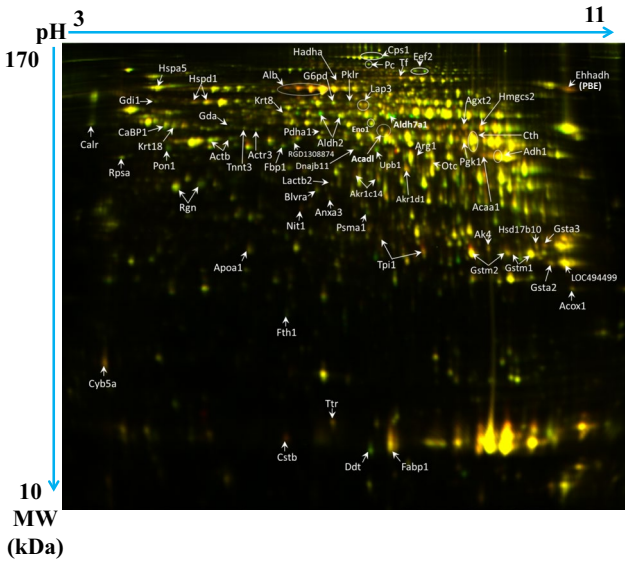

Fig. 3 Representative 2D-DIGE merged image of protein expression in the livers of SD rats untreated and treated with TCE. Proteins extracted from rats in the control and those in the TCE (500 mg/kg) treatment were differentially labeled with Cy3 in green and Cy5 in red (a merged spot would appear yellow)

hepatotoxicity. Their levels were evaluated by Western-blot analysis. Aldh2 was down-regulated in the livers of the rats exposed to TCE for 14 days at doses of 250 and 1000 mg/kg (Fig. 6), while Gstm1 was up-regulated at doses of 500 and 1000 mg/kg. PBE was significantly up-regulated by TCE at doses of 500 and 1000 mg/kg. PBE was the only protein that demonstrated TCE dose-dependent enhancement of expression in the livers of rats.

Discussion

Following exposure of SD rats to TCE by gastric gavage (for 14 days), significant increases in the liver index and the activities of liver damage marker enzymes (ALT, AST and ALP) were observed. This indicates that rats, in addition to mice, are vulnerable to TCE-induced liver injury. Furthermore, albumin and total protein in serum were decreased after treatment of TCE. Albumin in serum is mainly produced by the liver. Moreover, liver is also the major organ where TCE is metabolized for hepatotoxicity. The active metabolites of TCE may impair hepatocellular function and

Table 2 Statistical data and MALDI-TOF MS/MS identification results of differentially expressed proteins

Gene name[a]	Protein name	Swiss-Prot_ID[b]	Theoretical M_W (Da)/pI[c]	1-ANOVA[d]	Average ratio and t test[e]			Mascot score[f]	MS Coverage[g]
					250 mg/kg TCE vs control	500 mg/kg TCE vs control	1000 mg/kg TCE vs control		
(A) Fatty acid metabolism ($p = 1.84E-11$)									
Acaa1	3-Ketoacyl-CoA thiolase A, peroxisomal	THIKA_RAT	44,319/9.6	0.0074	–	1.46*	1.41*	125	7
Acadl[h]	Long-chain specific acyl-CoA dehydrogenase, mitochondrial	ACADL_RAT	48,242/8.7	0.0011	–	1.27*	1.32*	58	5
				2.5E−05	1.65*	1.95**	2.1**	108	8
Acox1	Peroxisomal acyl-coenzyme A oxidase 1	ACOX1_RAT	75,030/9.2	0.0002	1.49**	1.47**	1.66*	337	8
Adh1	Alcohol dehydrogenase 1	ADH1_RAT	40,532/9.7	2.5E−05	1.33*	1.37**	1.38**	112	5
Aldh2[h]	Aldehyde dehydrogenase, mitochondrial	ALDH2_RAT	56,966/6.8	1.1E−05	−1.39*	−1.64**	−1.58**	149	10
				0.00001	−1.65**	−1.98**	−2**	392	12
Aldh7a1	Alpha-aminoadipic semialdehyde dehydrogenase	AL7A1_RAT	59,225/9	0.039	–	–	−1.36*	132	5
Eci	3,2-*Trans*-enoyl-CoA isomerase, mitochondrial	ECI1_RAT	32,348/10.1	9.2E−06	1.68*	1.79**	1.86**	285	13
PBE (Ehhadh)	Peroxisomal bifunctional enzyme	ECHP_RAT	79,179/9.9	0.00049	1.7*	1.84**	2.04**	252	10
Hadha	Trifunctional enzyme subunit alpha, mitochondrial	ECHA_RAT	83,297/9.8	0.019	1.15*	1.27*	1.26*	84	6
(B) PPAR signaling pathway ($p = 1.24E-05$)									
Fabp1	Fatty acid-binding protein, liver	FABPL_RAT	14,320/9	0.0031	1.31*	1.26*	1.37*	277	36
Hmgcs2	Hydroxymethylglutaryl-CoA synthase, mitochondrial	HMCS2_RAT	57,332/9.5	0.002	1.32*	1.32*	1.37**	217	12
Proteins also participated in the above pathway/pathways: Acaa1, Acadl, Acox1, Ehhadh									
(C) Glycolysis/gluconeogenesis ($p = 1.56E-10$)									
Eno1	Alpha-enolase	ENOA_RAT	47,440/6.2	0.00042	−1.13*	−1.22*	−1.2*	157	8
Fbp1	Fructose-1,6-bisphosphatase 1	F16P1_RAT	40,040/5.4	0.0062	−1.18*	−1.32**	−1.27*	158	6
Pc	Pyruvate carboxylase, mitochondrial	PYC_RAT	130,436/6.4	0.01	–	−1.3*	−1.4*	366	8

Table 2 (continued)

Gene name[a]	Protein name	Swiss-Prot_ID[b]	Theoretical M_W (Da)/pI[c]	1-ANOVA[d]	Average ratio and t test[e]			Mascot score[f]	MS Coverage[g]
					250 mg/kg TCE vs control	500 mg/kg TCE vs control	1000 mg/kg TCE vs control		
Pdha1	Pyruvate dehydrogenase E1 component subunit alpha, somatic form, mitochondrial	ODPA_RAT	43,883/9.4	0.0075	1.37*	1.49*	–	48	5
Pgk1	Phosphoglycerate kinase 1	PGK1_RAT	44,909/9	8.8E−05	1.31**	1.29**	1.22**	91	7
Pklr	Pyruvate kinase isozymes R/L	KPYR_RAT	62,504/6.5	0.0059	–	1.27*	1.3*	106	5
Tpi1[h]	Triosephosphate isomerase	TPIS_RAT	27,345/7.7	8.9E−05	1.31*	1.53*	1.65**	346	28
				1.7E−06	1.31*	1.68**	1.81**	142	13
(D) Glutathione metabolism ($p = 4.06E-08$)									
G6pd	Glucose-6-phosphate 1-dehydrogenase	G6PD_RAT	59,794/5.9	0.032	–	1.26*	1.25*	61	5
Gsta1	Glutathione *S*-transferase alpha-1	GSTA1_RAT	25,705/9.5	1.4E−05	1.4*	1.56**	1.65**	223	17
Gsta3	Glutathione *S*-transferase alpha-3	GSTA3_RAT	25,360/9.3	0.0025	1.3*	1.29*	1.48*	152	14
Gstm1[h]	Glutathione *S*-transferase Mu 1	GSTM1_RAT	26,068/9	2.8E−05	1.37*	1.56**	1.75**	211	26
				4.4E−05	1.29*	1.46**	1.54**	264	30
Gstm2[h]	Glutathione *S*-transferase Mu 2	GSTM2_RAT	25,857/7.7	1.5E−05	1.39*	1.58**	1.67**	222	26
				0.00024	1.31*	1.42**	1.5**	313	26
LOC494499	Glutathione *S*-transferase alpha-2	GSTA2_RAT	25,657/9.5	0.00021	1.33**	1.38**	1.43**	197	17
(E) Amino acid metabolism									
Lap3[h]	Cytosol aminopeptidase	AMPL_RAT	56,514/6.9	0.031	1.34*	1.38*	1.4*	91	5
				0.018	–	1.31*	1.29*	162	9
(1) Valine, leucine and isoleucine degradation ($p = 3.48E-08$)									
Hsd17b10	3-Hydroxyacyl-CoA dehydrogenase type-2	HCD2_RAT	27,343/9.7	0.00021	1.21*	1.26**	1.33**	299	20
Proteins also participated in the above pathway/pathways: Acaa1, Aldh2, Aldh7a1, Ehhadh, Hadha, Hmgcs2									
(2) Arginine and proline metabolism ($p = 1.54E-06$)									
Arg1	Arginase-1	ARGI1_RAT	35,122/6.9	3.5E−06	1.13*	1.23**	1.25**	154	8
Otc	Ornithine carbamoyltransferase, mitochondrial	OTC_RAT	39,918/9.6	3.8E−05	1.23*	1.34**	1.46**	311	14
Cps1[h]	Carbamoyl-phosphate synthase, mitochondrial	CPSM_RAT	165,673/6.3	0.022	–	–	−1.58*	387	5
				0.0072	–	−1.48*	−1.62*	362	5
				0.026	–	−1.33*	−1.47*	462	5

Table 2 (continued)

Gene name[a]	Protein name	Swiss-Prot_ID[b]	Theoretical M_W (Da)/pI[c]	1-ANOVA[d]	Average ratio and t test[e]			Mascot score[f]	MS Coverage[g]
					250 mg/kg TCE vs control	500 mg/kg TCE vs control	1000 mg/kg TCE vs control		
Proteins also participated in the above pathway/pathways: Aldh2, Aldh7a1, Lap3									
(3) Glycine, serine and threonine metabolism ($p = 1.25E{-}03$)									
Agxt2	Alanine–glyoxylate aminotransferase 2, mitochondrial	AGT2_RAT	57,905/9.3	6.5E−05	1.31*	1.23*	1.28**	72	6
Cth[h]	Cystathionine gamma-lyase	CGL_RAT	44,262/9.3	0.0017	1.22*	1.24*	1.24*	245	14
				0.0014	1.19*	1.28*	1.22*	343	17
(F) Porphyrin and chlorophyll metabolism ($p = 2.09E{-}02$)									
Blvra	Biliverdin reductase A	BIEA_RAT	33,716/5.8	0.029	–	−1.29*	−1.25*	214	18
Fth1	Ferritin heavy chain	FRIH_RAT	21,284/5.9	0.015	−1.42*	−1.41*	−1.51*	310	26
(G) Other proteins									
(1) Chaperone proteins									
Hspd1[h]	60 kDa heat shock protein, mitochondrial	CH60_RAT	61,088/5.8	4.7E−05	1.25*	1.43**	1.44**	218	10
				0.0025	–	1.26*	1.23*	544	12
CaBP1	Protein disulfide-isomerase A6	PDIA6_RAT	48,542/4.9	0.0018	−1.27*	−1.28*	−1.27*	329	18
Calr	Calreticulin	CALR_RAT	48,137/4.2	0.026	–	−1.39*	−1.22*	160	8
Dnajb11	DnaJ homolog subfamily B member 11	DJB11_RAT	40,755/5.9	0.0022	−1.19*	−1.24*	−1.25*	101	7
Hspa5	78 kDa glucose-regulated protein	GRP78_RAT	72,473/4.9	0.0046	−1.31*	−1.39*	−1.45*	343	8
(2) Protein synthesis/degradation									
Cstb	Cystatin-B	CYTB_RAT	11,303/5.9	7.8E−06	1.57**	1.58**	1.69**	141	21
Lactb2	Beta-lactamase-like protein 2	LACB2_RAT	32,749/5.9	0.0038	1.21*	1.21*	1.31*	301	18
Eef2[h]	Elongation factor 2	EF2_RAT	96,192/6.4	0.00018	−1.51*	−1.53*	−1.47*	332	10
				0.00048	−1.19*	−1.22*	−1.25**	263	8
Psma1	Proteasome subunit alpha type-1	PSA1_RAT	29,784/6.2	0.00034	−1.25**	−1.26**	−1.2**	108	9
Rpsa	40S ribosomal protein SA	RSSA_RAT	32,917/4.6	0.009	−1.22*	−1.24**	−1.23*	337	20
(3) Cytoskeletal proteins									
Actb[h]	Actin, cytoplasmic 1	ACTB_RAT	42,052/5.2	0.0058	–	−1.39*	−1.32*	223	13
				0.01	–	−1.29*	−1.33*	266	12
Actr3	Actin-related protein 3	ARP3_RAT	47,783/5.5	2.1E−05	−1.81*	−2.22**	−2.36**	256	14
Krt8	Keratin, type II cytoskeletal 8	K2C8_RAT	53,985/5.7	0.0064	–	−1.17*	−1.22*	354	16

Table 2 (continued)

Gene name[a]	Protein name	Swiss-Prot_ID[b]	Theoretical M_W (Da)/pI[c]	1-ANOVA[d]	Average ratio and t test[e]			Mascot score[f]	MS Coverage[g]
					250 mg/kg TCE vs control	500 mg/kg TCE vs control	1000 mg/kg TCE vs control		
Krt18	Keratin, type I cytoskeletal 18	K1C18_RAT	47,732/5	1.6E−05	− 1.3*	− 1.44**	− 1.45**	267	17
Tnnt3	Troponin T, fast skeletal muscle	TNNT3_RAT	30,732/6.2	0.0014	− 1.23*	− 1.28*	− 1.29*	102	6
(4) Serum transport-related proteins									
Alb[h]	Serum albumin	ALBU_RAT	70,682/6.1	0.00043	1.64*	1.66*	1.44*	445	17
				0.00013	1.67*	1.74**	1.53*	535	17
				7.5E−05	1.66**	1.68**	1.5*	526	16
				0.0011	1.49*	1.47*	1.28*	538	16
Apoa1	Apolipoprotein A-I	APOA1_RAT	30,100/5.4	0.0021	1.33*	1.23*	1.16*	120	11
Tf	Serotransferrin	TRFE_RAT	78,512/7.8	0.019	–	1.35*	1.3*	262	10
Ttr	Transthyretin	TTHY_RAT	15,824/5.7	0.02	–	1.37*	1.43*	82	8
(5) Redox-related proteins									
Akr1d1	3-Oxo-5-beta-steroid 4-dehydrogenase	AK1D1_RAT	37,639/6.2	0.025	–	–	1.25*	209	15
Akr1c14[h]	3-Alpha-hydroxysteroid dehydrogenase	DIDH_RAT	37,517/6.8	0.0025	1.22*	1.28*	1.33**	98	11
				0.0084	1.16*	1.16*	1.23**	233	17
Cyb5a	Cytochrome b5	CYB5_RAT	15,346/4.7	0.047	–	1.29*	1.31*	484	47
(6) Lyases									
Upb1	Beta-ureidopropionase	BUP1_RAT	44,584/6.5	0.0015	1.21*	1.28*	1.28*	254	17
Ddt	D-dopachrome decarboxylase	DOPD_RAT	13,239/6.1	7.3E−06	− 1.5*	− 1.73**	− 1.74**	208	28
Gda	Guanine deaminase	GUAD_RAT	51,554/5.5	0.0016	− 1.27*	− 1.3*	− 1.32*	145	12
(7) Hydrolases and related proteins									
Nit1	Nitrilase homolog 1	NIT1_RAT	32,697/5.9	9.90E−10	1.81**	1.85**	2.01**	273	19
Anxa3	Annexin A3	ANXA3_RAT	36,569/5.9	0.0035	− 1.29*	− 1.47*	− 1.35*	249	12
Pon1	Serum paraoxonase/arylesterase 1	PON1_RAT	39,699/5	0.00022	− 1.43*	− 1.56*	− 1.61*	154	7
RGD1308874	Adipocyte plasma membrane-associated protein	APMAP_RAT	42,207/5.5	6.1E−05	− 1.17*	− 1.32**	− 1.36**	121	10
Rgn[h]	Regucalcin	RGN_RAT	33,939/5.1	0.039	–	− 1.46*	− 1.44*	287	21
				0.00034	− 1.19*	− 1.33**	− 1.37**	349	24

Table 2 (continued)

Gene name[a]	Protein name	Swiss-Prot_ID[b]	Theoretical M_W (Da)/pI[c]	1-ANOVA[d]	Average ratio and t test[e]			Mascot score[f]	MS Coverage[g]
					250 mg/kg TCE vs control	500 mg/kg TCE vs control	1000 mg/kg TCE vs control		
(8) Kinase and related proteins									
Ak4	Adenylate kinase isoenzyme 4, mitochondrial	KAD4_RAT	25,301/8.9	0.00039	1.38**	1.45**	1.59*	193	22
Gdi1	Rab GDP dissociation inhibitor alpha	GDIA_RAT	51,074/4.9	0.000068	− 1.17*	− 1.21**	− 1.26**	355	23
RGD1303003	ES1 protein homolog, mitochondrial	ES1_RAT	28,497/10	0.00037	1.24*	1.21*	1.28**	190	13

[a]Gene names of the identified proteins corresponded to the specific spots as indicated in Fig. 3

[b]Protein ID was accessed from Swiss-Prot database by data searching

[c]Theoretical MW and pI were accessed from UniProt database

[d]p values were calculated by one-way ANOVA analysis

[e]Average ratios of spot abundance of TCE-induced samples relative to controls are shown

[f]A p value from Student's t test was given as a measure of the confidence for the ratio of each spot in a TCE group to that in the control, and the asterisks (*$p < 0.05$ and **$p < 0.001$) indicate a significant difference between a TCE-treated group and the control group. Protein hit statistics from Mascot search engine are detailed, including the probability-based log-Mascot score

[g]The percentage of protein sequence coverage

[h]Some spots with the same trend (up or down-regulated) were identified as the same proteins, which explains why an average ratio fold change of ± 1.2 and $p < 0.05$ was considered as a significant change

decrease albumin synthesis, which contributes to the reduction of albumin in serum (Carvalho and Verdelho Machado 2018; Alves de Mattos 2011). Because albumin is the most abundant protein in serum, its reduction usually leads to a drop of the total protein in serum.

Quantitative analysis by proteomic approaches suggested that the expression levels of 66 individual proteins were altered in the livers of TCE-treated rats. Bioinformatic analysis revealed that many of these proteins are metabolic enzymes mainly participating in glycolysis and the metabolism of lipids and glutathione. This result is consistent with other studies (Lash et al. 2014). The levels of 6 proteins, among 39 different proteins enhanced for expression, were further verified by Western blot analysis. After functional analysis, the six proteins were involved in different biological processes associated with liver injury or hepatic carcinogenesis (Puri 2019; He et al. 2020; Seo et al. 2019; Park et al. 2019; Yu et al. 2018; Gao et al. 2018; Panisello-Rosello 2018; Koen et al. 2016; Kumar et al. 2009). Thus, these proteins were selected for further verification. Of these proteins, the levels of Eno1, Ddt and Cps1 did not change; Aldh2 and Gstm1 were down- and up-regulated, respectively, without a typical dose–response relationship. However, the expression of PBE increased in a dose-dependent manner in the livers of rats exposed to TCE.

Aldh2 is the main enzyme responsible for acetaldehyde oxidation in ethanol metabolism, which implies that its down-regulation in the livers of rats by TCE may increase the oxidative burdens in the body and potentially inhibit ethanol metabolism. This observation is consistent with

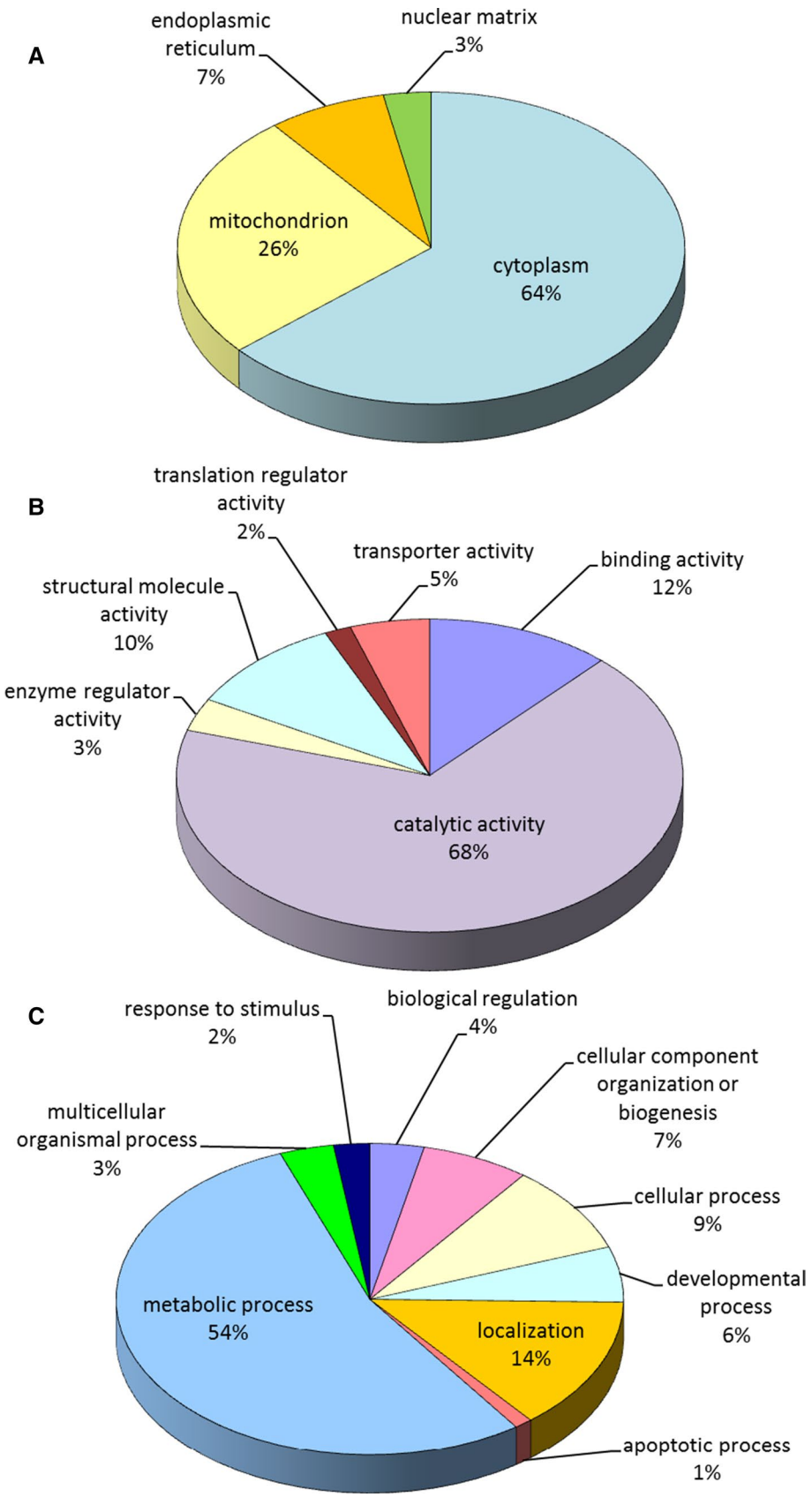

Fig. 4 Functional classification of TCE-induced differential proteomic profiles according to their cellular localization (**a**), molecular function (**b**) and biological processes (**c**). The classification was conducted using the PANTHER classification system

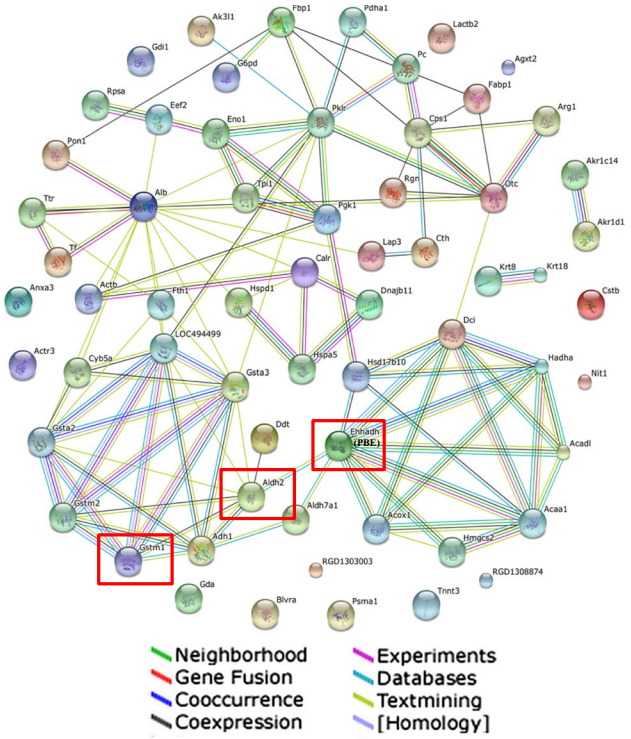

Fig. 5 Protein interaction networks of TCE-induced differential proteomic profiles. The networks were generated with STRING database for direct physical and indirect functional protein interaction analysis (PBE is also named Ehhadh)

previous reports demonstrating induction of oxidative stress in the liver of mice by TCE (Atkinson et al. 1993) and decreased expression of Aldh2 and its enzymatic activity (Wang et al. 2010). Gstm1 (a critical enzyme for glutathione (GSH) metabolism) was up-regulated in the livers of rats exposed to TCE. A major function of GSH in mammalian cells is to attenuate oxidative stress, a factor implicated in cancer development and progression (Watanabe and Nagashima 1983). Thus, enhanced expression of Gstm1 might mediate multiple pathologic processes, such as the liver injury induced by TCE.

PBE is a bifunctional enzyme, which has two functional domains, the N-terminal region with enoyl-CoA hydratase activity and the C-terminal region with 3-hydroxyacyl-CoA dehydrogenase activity (Uchida et al. 1992). It is one of the four enzymes in the peroxisomal β-oxidation pathway. PBE is indispensable for the production of medium-chain dicarboxylic acids, which are essential for the coordinated induction of mitochondrial and peroxisomal oxidative pathways during fasting (Houten et al. 2012). Deficiency of this protein can cause peroxisomal disorders such as Zellweger syndrome (Itoh et al. 2000). PBE is also a potential biomarker for hepatocellular carcinoma, as indicated by high-throughput RNA-seq analysis (Gao et al. 2018; Jiang et al. 2019). PBE binds and activates the activation function-1 region of PPARα, a nuclear receptor associated with hepatotoxicity (Juge-Aubry et al. 2001). Interestingly, TCE-induced liver toxicity and carcinogenesis are also mediated partly by activation of PPARα (Mandard et al. 2004; Kyrklund et al. 1983; Klaunig et al. 2003). Therefore, the enhanced expression of PBE in the livers of rats exposed to TCE is likely induced via activation of PPARα by TCE, and PBE may contribute to the hepatotoxicity of TCE.

In summary, the results of this study indicate that TCE induces liver injury in rats. In this model, the expression of 66 liver proteins was altered, among which, PBE, a peroxisomal bifunctional enzyme, can be enhanced for expression, possibly in response to oxidative stress caused by TCE exposure. The role of PBE in TCE-induced liver injury is worth further investigation.

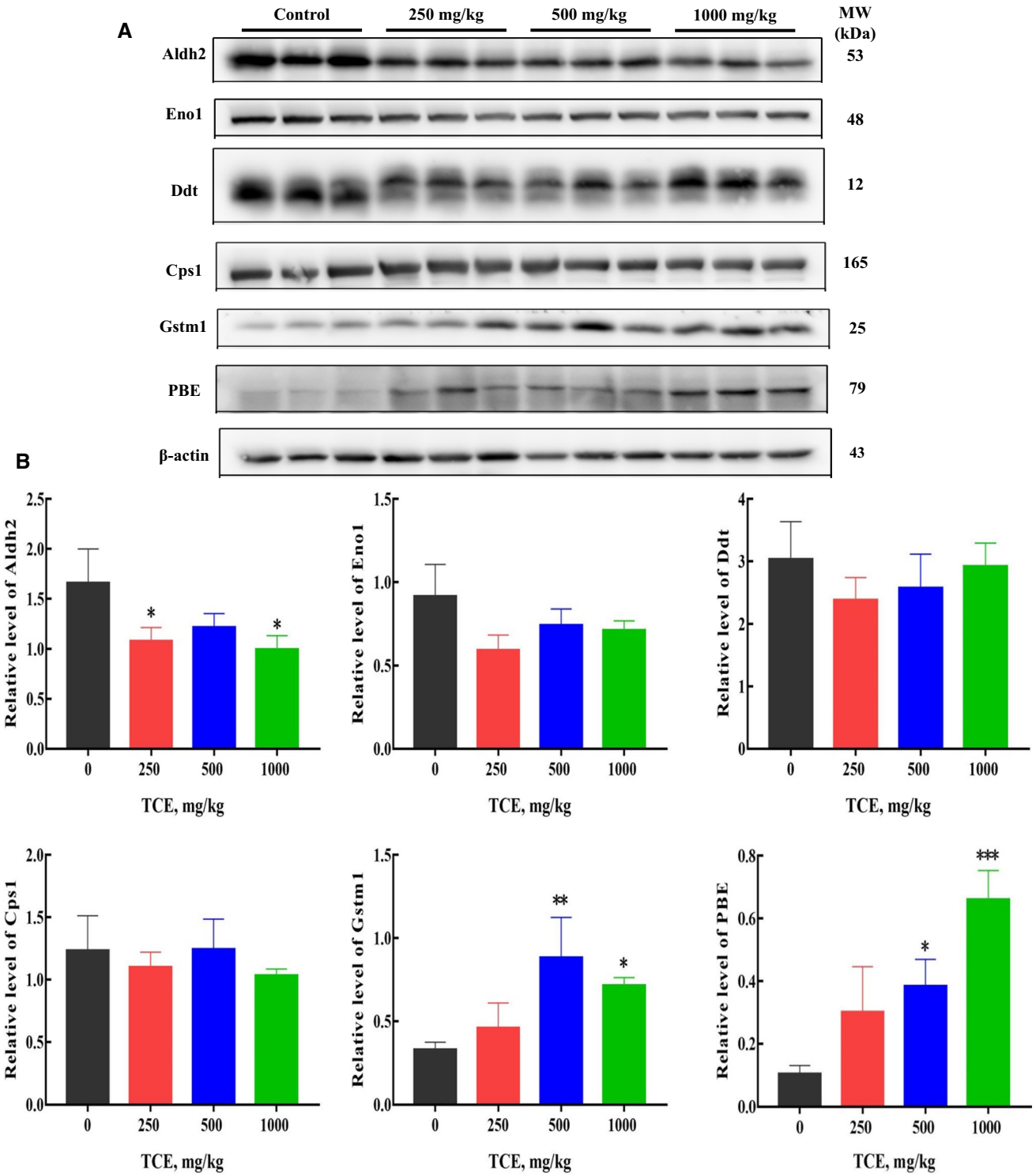

Fig. 6 Verification of TCE-targeted proteins in the rat liver. The levels of identified proteins in the liver samples from three rats in each group were confirmed by Western blot analysis. β-Actin was used as the loading control. **a** Protein bands of Aldh2, Eno1, Ddt, Cps1, Gstm1, and PBE. **b** Relative levels of Aldh2, Eno1, Ddt, Cps1, Gstm1, and PBE. Data are means and SD of three replicates; $*p<0.05$, $**p<0.01$, $***p<0.001$, compared with the control

Acknowledgements This work was supported by the National Natural Science Foundation of China (NSFC) (No. 81872666), and Sanming Project of Medicine in Shenzhen (No. SZSM201611090).

Author contributions Nuanyuan Luo and Qunqun Chang analyzed the data and performed statistical tests. Nuanyuan Luo wrote the manuscript. Peiwu Huang extracted protein and conducted 2D-DIGE. Xiaohu Ren conducted protein quantitation and identification. Wei Liu measured Serum biochemical index. Li Zhou and Peiwu Huang were responsible for animal treatment. Yungang Liu revised the manuscript and provided technical support. Jianjun Liu designed the study and provided technical support. All authors have read and approved the manuscript.

Compliance with ethical standards

Conflict of interest The authors do not have any conflicts of interest or financial interests to disclose.

Animal rights All experimental procedures about animal treatment and sample collection were conducted according to the Institutional Animal Care Guidelines and the animal experiments were approved by the committee of ethnics in the Shenzhen Center for Disease Control and Prevention.

References

Allemand H et al (1978) Metabolic activation of trichloroethylene into a chemically reactive metabolite toxic to the liver. J Pharmacol Exp Ther 204:714–723

Alves de Mattos A (2011) Current indications for the use of albumin in the treatment of cirrhosis. Ann Hepatol 10(Suppl 1):S15–S20

Atkinson A, Meeks RG, Roy D (1993) Increased oxidative stress in the liver of mice treated with trichloroethylene. Biochem Mol Biol Int 31:297–304

Bergmeyer HU, Scheibe P, Wahlefeld AW (1978) Optimization of methods for aspartate aminotransferase and alanine aminotransferase. Clin Chem 24:58–73

Carvalho JR, Verdelho Machado M (2018) New insights about albumin and liver disease. Ann Hepatol 17:547–560

Chiu WA et al (2013) Human health effects of trichloroethylene: key findings and scientific issues. Environ Health Perspect 121:303–311

Franceschini A et al (2013) STRING v9.1: protein–protein interaction networks, with increased coverage and integration. Nucleic Acids Res 41:D808–D815

Gao X, Wang X, Zhang S (2018) Bioinformatics identification of crucial genes and pathways associated with hepatocellular carcinoma. Biosci Rep 38 (2018)

He J et al (2020) Screening of significant biomarkers related with prognosis of liver cancer by lncRNA-associated ceRNAs analysis. J Cell Physiol 235:2464–2477

Houten SM et al (2012) Peroxisomal L-bifunctional enzyme (Ehhadh) is essential for the production of medium-chain dicarboxylic acids. J Lipid Res 53:1296–1303

Huang HY et al (2009) An investigation of hormesis of trichloroethylene in L-02 liver cells by differential proteomic analysis. Mol Biol Rep 36:2119–2129

Itoh M et al (2000) Developmental and pathological expression of peroxisomal enzymes: their relationship of d-bifunctional protein deficiency and Zellweger syndrome. Brain Res 858:40–47

Jiang W et al (2019) Identification of the pathogenic biomarkers for hepatocellular carcinoma based on RNA-seq analyses. Pathol Oncol Res 25:1207–1213

Juge-Aubry CE, Kuenzli S, Sanchez JC, Hochstrasser D, Meier CA (2001) Peroxisomal bifunctional enzyme binds and activates the activation function-1 region of the peroxisome proliferator-activated receptor alpha. Biochem J 353:253–258

Kamijima M, Hisanaga N, Wang H, Nakajima T (2007) Occupational trichloroethylene exposure as a cause of idiosyncratic generalized skin disorders and accompanying hepatitis similar to drug hypersensitivities. Int Arch Occup Environ Health 80:357–370

Khan S et al (2009) Effect of trichloroethylene (TCE) toxicity on the enzymes of carbohydrate metabolism, brush border membrane and oxidative stress in kidney and other rat tissues. Food Chem Toxicol 47:1562–1568

Klaunig JE et al (2003) PPARalpha agonist-induced rodent tumors: modes of action and human relevance. Crit Rev Toxicol 33:655–780

Koen YM, Galeva NA, Metushi IG, Uetrecht J, Hanzlik RP (2016) Protein targets of isoniazid-reactive metabolites in mouse liver in vivo. Chem Res Toxicol 29:1064–1072

Kumar M et al (2009) Study of genetic polymorphism in solvent exposed population and its correlation to in vitro effect of trichloroethylene on lymphocytes. J Environ Biol 30:685–691

Kyrklund T, Alling C, Haglid K, Kjellstand P (1983) Chronic exposure to trichloroethylene: lipid and acyl group composition in gerbil cerebral cortex and hippocampus. Neurotoxicology 4:35–42

Lash LH, Fisher JW, Lipscomb JC, Parker JC (2000) Metabolism of trichloroethylene. Environ Health Perspect 108(Suppl 2):177–200

Lash LH, Chiu WA, Guyton KZ, Rusyn I (2014) Trichloroethylene biotransformation and its role in mutagenicity, carcinogenicity and target organ toxicity. Mutat Res Rev Mutat Res 762:22–36

Liu J et al (2007) Comparative proteomic analysis on human L-02 liver cells treated with varying concentrations of trichloroethylene. Toxicol Ind Health 23:91–101

Mandard S, Muller M, Kersten S (2004) Peroxisome proliferator-activated receptor alpha target genes. Cell Mol Life Sci 61:393–416

Panisello-Rosello A et al (2018) Aldehyde dehydrogenase 2 (ALDH2) in rat fatty liver cold ischemia injury. Int J Mol Sci 19

Park MJ et al (2019) Constitutive release of CPS1 in bile and its role as a protective cytokine during acute liver injury. Proc Natl Acad Sci USA 116:9125–9134

Puri L et al (2019) GSTM1 and liver iron content in children with sickle cell anemia and iron overload. J Clin Med 8

Sano Y et al (2009) Trichloroethylene liver toxicity in mouse and rat: microarray analysis reveals species differences in gene expression. Arch Toxicol 83:835–849

Seo W et al (2019) ALDH2 deficiency promotes alcohol-associated liver cancer by activating oncogenic pathways via oxidized DNA-enriched extracellular vesicles. J Hepatol 71:1000–1011

Uchida Y, Izai K, Orii T, Hashimoto T (1992) Novel fatty acid beta-oxidation enzymes in rat liver mitochondria II Purification and properties of enoyl-coenzyme A (CoA) hydratase/3-hydroxyacyl-CoA

dehydrogenase/3-ketoacyl-CoA thiolase trifunctional protein. J Biol Chem 267:1034–1041
Wang J et al (2010) Inhibition of aldehyde dehydrogenase 2 by oxidative stress is associated with cardiac dysfunction in diabetic rats. Mol Med 17:172
Watanabe A, Nagashima H (1983) Glutathione metabolism and glucose 6-phosphate dehydrogenase activity in experimental liver injury. Acta Med Okayama 37:463–470
Wu C, Schaum J (2000) Exposure assessment of trichloroethylene. Environ Health Perspect 108(Suppl 2):359–363
Xu XY et al (2012) Altered expression of hepatic metabolic enzyme and apoptosis-related gene transcripts in human hepatocytes treated with trichloroethylene. Hum Exp Toxicol 31:861–867
Yu S et al (2018) A novel lncRNA, TCONS_00006195, represses hepatocellular carcinoma progression by inhibiting enzymatic activity of ENO1. Cell Death Dis 9:1184